

# Selective Interactions Between 5-fluorouracil Prodrug Enantiomers and DNA Investigated with Voltammetry and Molecular Docking Simulation

Bao Cheng, Xiao-Qing Cai, Qian Miao, Zuo-Hui Wang, Mao-Lin Hu\*

College of Chemistry and Materials Engineering, Wenzhou University, Wenzhou 325035, China

\*E-mail: [maolin\\_hucn@yahoo.com](mailto:maolin_hucn@yahoo.com)

Received: 24 October 2013 / Accepted: 29 December 2013 / Published: 2 February 2014

---

The selective interactions between 5-fluorouracil prodrug enantiomers [(R)-A/(S)-A] and DNA were investigated through cyclic voltammetry and molecular docking simulation. The investigation indicates that interactions between (R)-A/(S)-A and DNA helix can be considered as groove binding. To characterize the binding ability of (R)-A/(S)-A with DNA, binding constants and binding free energies were obtained via voltammetric data and AMBER software, which illustrate that the DNA more selectively binds to (R)-A. For the binding strength, the computational results complement experimental measurements. This study serves as a good reference for the rational design and screening of enantiomer prodrugs of 5-fluorouracil.

---

**Keywords:** Selective interactions; Enantiomer prodrugs; Cyclic voltammetry; Molecular docking simulation; Binding constant.

## 1. INTRODUCTION

The study of the selective interactions of small molecules (often termed as drugs or ligands) with DNA has been an important topic for decades. [1,2] A variety of analytical techniques have been developed for characterization and identification of the interactions between DNA and small molecules with relative advantages and disadvantages.[3,4] Unfortunately, most of these methods suffer from high cost, low sensitivity and procedural complication. To date, electrochemical methods, especially cyclic voltammetry (CV) technique, appear to be much more elegant for use in exploring those interactions because of its simplicity, high sensitivity and low cost, which is expected to yield quantitative information.[5,6]

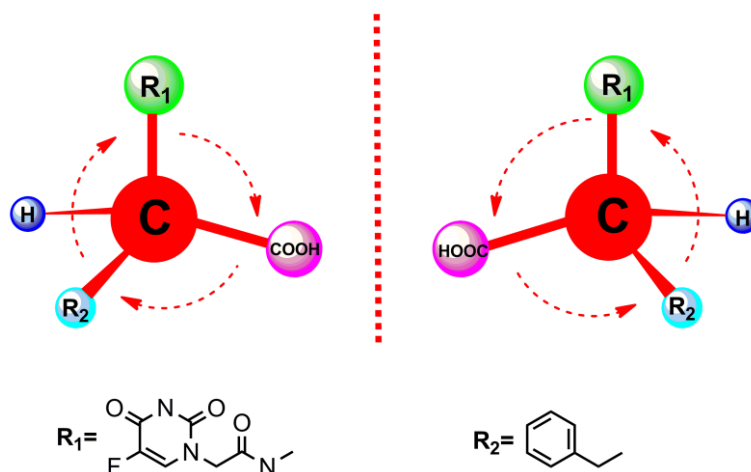
Molecular docking simulation also plays an important role in rational drug design and has been applied to describe the most probable mode of drug-DNA binding. When being used prior to experimental screening, DOCK, AutoDock and molecular operating environment (MOE) are able to

accurately predict the structure of drug–DNA complexes, [7] and enable a great reduction in the cost and labour required for the development of new potent medicinal drugs.[8] Docking techniques are expected to an increasingly important part in drug discovery.[9]

Heidelberger and colleagues found 5-fluorouracil has anti-cancer effect,[10] which has been widely used in the treatment of solid malignant tumours.[11] However, because of the poor tumor selectivity and high incidence of toxicity in the bone marrow and gastrointestinal tract, many 5-fluorouracil based prodrugs have been synthesized in order to improve the topical delivery and reduce the side effects.[12] Although 5-fluorouracil and DNA interact via intercalation,[13] the modes of interactions of its prodrugs with DNA could be different. In order to determine the unknown modes of the interactions, in this work (R)-A/(S)-A were synthesised and CVs were carried out. The docking behaviour of (R)-A/(S)-A with DNA was examined using both experimental and theoretical methods. In addition, the structure-activity relationship was explained through calculating the binding free energies using the AMBER software. [14] The theoretical data are in good agreement with the experimental results, which is absolutely significant to the rational design and effective screening of new drugs.

## 2. EXPERIMENTAL

### 2.1. Apparatus and reagents



**Scheme 1.** Molecular structures of the 5-fluorouracil enantiomer prodrugs [(R)-A/(S)-A].

Calf thymus DNA (CT-DNA) from Sigma Chemical Co. was used as received, since the purity was sufficiently high as determined by the optical measurement. [15] Except that the (R)-A/(S)-A (Scheme 1.) were synthesised in our laboratory according to a previously published method, [16] all other chemicals were purchased from Aldrich Chemical Company. The electrochemical experiments were carried out with a CHI 1030B electrochemical workstation (Shanghai Chenhua Co.).

## 2.2. Cyclic voltammetry

CT-DNA modified Au electrode was prepared as the following [17]: (i) a gold disk electrode (2mm in diameter) was first polished to a mirror finish with (1.0, 0.3 and 0.05  $\mu\text{m}$ ) alumina slurry successively and cleaned ultrasonically in ethanol and purified water; (ii) the electrode surface was scanned over the potential range from -0.2 to +1.5 V in 0.5 mol·L<sup>-1</sup> H<sub>2</sub>SO<sub>4</sub> until a constant characteristic voltammogram of a clean Au electrode was obtained; and (iii) the electrode was modified immediately by transferring 10  $\mu\text{L}$  of 1.0  $\mu\text{g}\cdot\mu\text{L}^{-1}$  DNA solution onto its surface, followed by drying in an N<sub>2</sub> stream. The DNA-modified gold electrode is denoted as CT-DNA/Au throughout this report. Voltammetric measurements were performed in a conventional three-electrode cell, with CT-DNA/Au as the working electrode, a saturated calomel electrode (SCE) as the reference electrode and a platinum wire as the auxiliary electrode. Typical CV experiments were conducted at room temperature (25 °C) in 5 mmol·L<sup>-1</sup> Fe(CN)<sub>6</sub><sup>3-/4-</sup> containing 0.05 mol·L<sup>-1</sup> Tris-HCl buffer solution of pH 7.3 and 0.1 mol·L<sup>-1</sup> KCl.

## 2.3. Molecular docking calculation

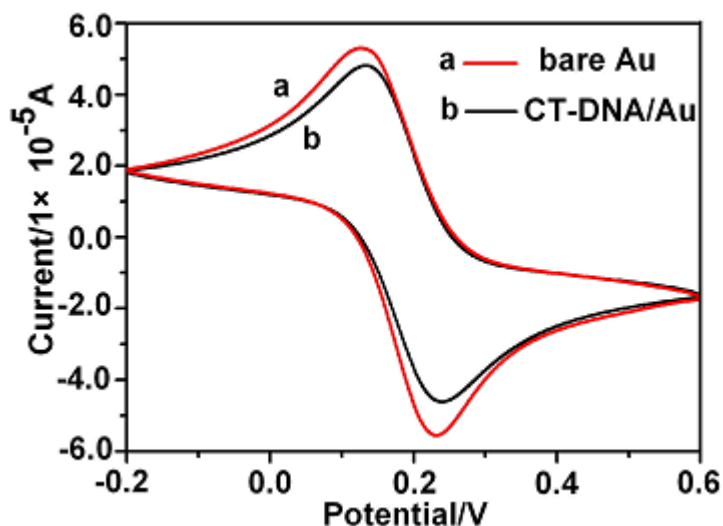
Docking simulations were performed using the AutoDock program package and the Lamarckian genetic algorithm (LGA) available in AutoDock 4.0, which has been proven to be most efficient, and reliable.[18] The LGA was used in this docking study of (R)-A/(S)-A with double-stranded DNA. The DNA duplex receptor structure was obtained from Protein Data Bank (PDB ID 2dyw) contained 12 base pairs. The base pair sequence was CGCGAATTCGCG: GCGCTTAAGCGC. All water molecules and ligands that co-crystallised with the DNA were removed from the original structure. The crystal structures of the (R)-A/(S)-A were obtained in our laboratory according to a previously published paper. [19] Then, the compounds and DNA were added along with Gasteiger charges and polar hydrogen atoms using AutoDockTools (ADT) version 1.5.2. We used AutoGrid 4.0 to calculate affinity grids centered on the active site. Under optimal conditions, we used grid maps with 80×60×110 points with a grid-point spacing of 0.375 Å. [20, 21] Only the flexibility of ligands was taken into account, and the rotatable bonds without resonance were allowed to rotate. Then, we began to conduct the molecular docking via the LGA using default parameters. For each ligand, fifty independent docking runs were carried out. The binding free energies of complex obtained from molecular docking calculation.

# 3. RESULTS AND DISCUSSION

## 3.1. Electrochemical measurements

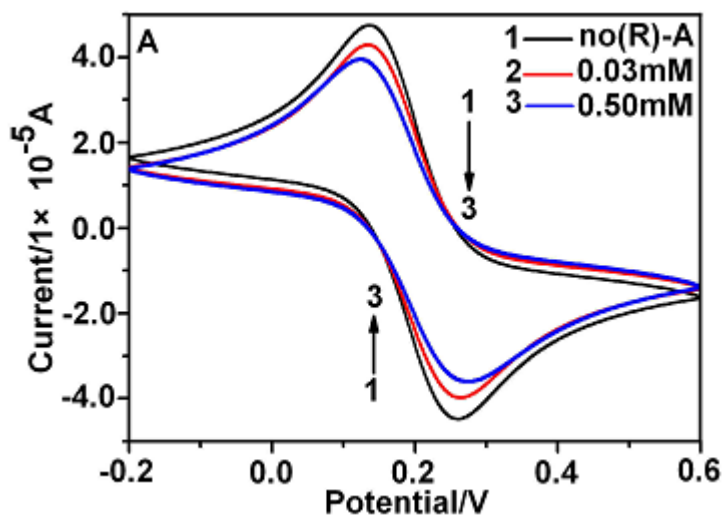
Fig. 1 presents the typical CV responses of Fe(CN)<sub>6</sub><sup>3-/4-</sup> at a bare Au and CT-DNA/Au electrode at the scan rate of 100 mV/s. Fe(CN)<sub>6</sub><sup>3-/4-</sup> produced a pair of well-defined redox waves at the bare Au ( curve a ) with a peak-to-peak separation of 98 mV. After the electrode was modified with

CT-DNA, there was an obvious decrease in the peak currents ( Fig. 1, curve b ), indicating that CT-DNA acted as the inert electron and mass transfer blocker to hinder the migration of ferricyanide towards the electrode surface. This demonstrates that CT-DNA has been successfully assembled on the Au surface. CVs remain stable after 20 scans in the Tris-HCl buffer solution, implicating the electrochemical stability of the CT-DNA film. [17, 20]



**Figure 1.** Cyclic voltammograms at a bare Au electrode (a) and CT-DNA/ Au (b) in  $5 \text{ mmol}\cdot\text{L}^{-1}$   $\text{Fe}(\text{CN})_6^{3-/4-}$  containing  $0.05 \text{ mol}\cdot\text{L}^{-1}$  Tris-HCl buffer solution of pH 7.3 and  $0.1 \text{ mol}\cdot\text{L}^{-1}$  KCl.

(R)-A/(S)-A are non-electroactive organic small molecules.  $\text{Fe}(\text{CN})_6^{3-/4-}$  was used as a redox probe to investigate the interactions of non-electroactive small molecules with CT-DNA. Fig. 2 shows the CV behaviors of the CT-DNA/Au electrode in the absence and presence of concentrations of (R)-A/(S)-A in  $5 \text{ mmol}\cdot\text{L}^{-1}$   $\text{Fe}(\text{CN})_6^{3-/4-}$  containing  $0.05 \text{ mol}\cdot\text{L}^{-1}$  Tris-HCl buffer solution of pH 7.3 and  $0.1 \text{ mol}\cdot\text{L}^{-1}$  KCl.



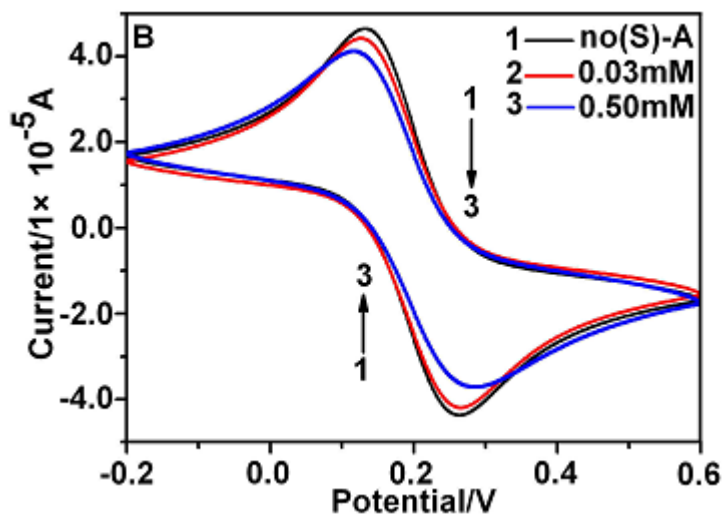


**Figure 2.** Cyclic voltammograms of the CT-DNA/Au electrode in the absence and presence of different concentrations of (R)-A (A) or (S)-A (B) in  $5 \text{ mmol}\cdot\text{L}^{-1} \text{ Fe(CN)}_6^{3-/4-}$  containing  $0.05 \text{ mol}\cdot\text{L}^{-1}$  Tris-HCl buffer solution of pH 7.3 and  $0.1 \text{ mol}\cdot\text{L}^{-1}$  KCl.

These experiments showed that both the redox peaks currents gradually decreased when solutions with different concentration from 0.03 to  $0.50 \text{ mmol}\cdot\text{L}^{-1}$  of (R)-A/(S)-A were investigated (some concentrations were omitted in Fig. 2A and Fig. 2B). Such a trend indicates that DNA films makes the redox process of  $\text{Fe(CN)}_6^{3-/4-}$  marker at the Au electrode more difficult due to the physical blockage as well as possible electrostatic repulsion. When (R)-A/(S)-A was added to the solution, they interacted with the coated DNA film to further hinder the transportation of the probe molecule toward the electrode surface.

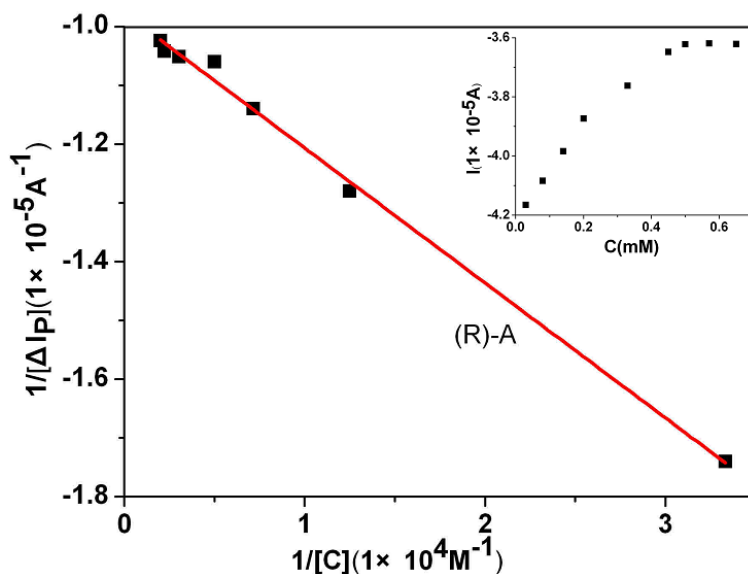


**Figure 3.** Plot the linear functional relationship between  $1/\Delta I_P$  and  $1/[C]$  for (R)-A. Inset: relations between oxidative peak currents and (R)-A concentration.

As a result, the redox peaks currents of  $\text{Fe}(\text{CN})_6^{3-/4-}$  decreased. Meanwhile, the oxidation peaks shifted toward a positive direction upon the addition of (R)-A/(S)-A. Such an observation indicates that the mode of interaction between (R)-A/(S)-A and CT-DNA helix could be considered as groove binding. [22]

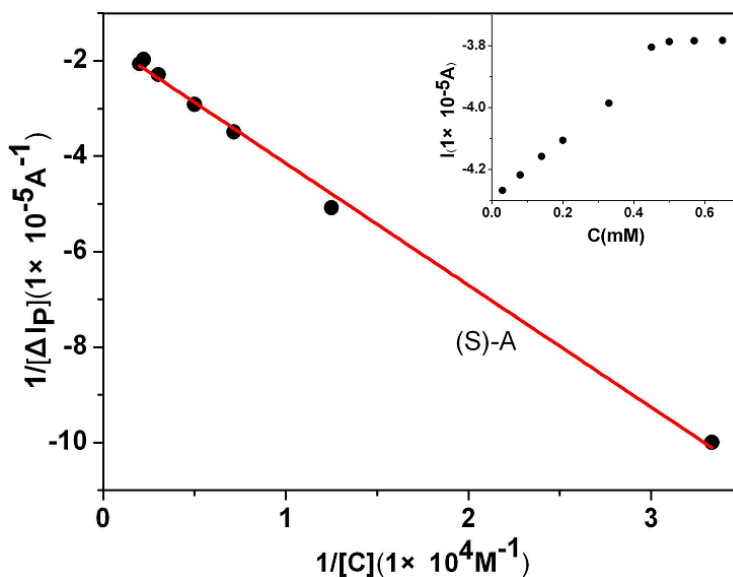


**Figure 4.** Plot the linear functional relationship between  $1/\Delta I_p$  and  $1/[C]$  for (S)-A. Inset: relations between oxidative peak currents and (S)-A concentration.

As can be seen from Fig. 3 and Fig. 4 (inserted Pictures), both the peak currents of the cyclic voltammograms decreased with increasing the concentrations of (R)-A/(S)-A and tended to achieve a saturation value, as expected for Langmuir adsorption behaviour. [23-25] For a quantitative comparison of the binding strength of (R)-A/(S)-A with CT-DNA, the binding constant ( $K$ ) between the test compounds and the CT-DNA were calculated, according to the Langmuir formula in Eq. (A.1). According to the method of Qu et al, [26] it is assumed that DNA and DRUG only produce a single complex  $\text{DNA} \cdot \text{DRUG}_m$ . The stoichiometric coefficient,  $m$ , and binding constant,  $K$ , between DRUG and DNA refer to the reaction scheme [2] for all-or-none (Hill) cooperativity of multiple ligand binding:



The condition of binding constant is as follows:

$$K[\text{DRUG}]^m = \frac{[\text{DNA} \cdot \text{DRUG}_m]}{[\text{DNA}]} = \frac{f}{1-f} \tag{2.1}$$

where  $f = \frac{[\text{DNA} \cdot \text{DRUG}_m]}{[\text{DNA}]_0}$  is the fraction of DNA to relative to the total DNA concentration

in the supporting electrolyte. Mass conservation dictates that:  $[\text{DNA}] = [\text{DNA}]_0 - [\text{DNA} \cdot \text{DRUG}_m]$ ,

then,

$$[\text{DRUG}] = [\text{DRUG}]_0 - m[\text{DNA} \cdot \text{DRUG}_m] \tag{2.2}$$

and

$$I = k' [\text{DRUG}] \tag{2.3}$$

$$\Delta I = I [\text{DNA}]_0 - I [\text{DRUG}] \tag{2.4}$$

where  $[\text{DRUG}]$  is the free concentration of  $[\text{DRUG}]$  and  $I [\text{DRUG}]$  is the peak current of  $[\text{DRUG}]$  in the presence of DNA.

Insertion of Eqs [2.2] and [2.3] into [2.4] yields:  
 $\Delta I = k' \cdot ([\text{DRUG}]_0 - [\text{DRUG}]) = k' \cdot m \cdot [\text{DNA} \cdot \text{DRUG}_m]$  [2.5]

and

$$\Delta I_{\text{max}} = k' \cdot m \cdot [\text{DNA}]_0 \tag{2.6}$$

$$\frac{\Delta I}{\Delta I_{\text{max}} - \Delta I} = \frac{[\text{DNA} \cdot \text{DRUG}_m]}{[\text{DNA}]_0 - [\text{DNA} \cdot \text{DRUG}_m]} = \frac{[\text{DNA} \cdot \text{DRUG}_m]}{[\text{DNA}]} \tag{2.7}$$

where  $\Delta I_{\text{max}}$  is the maximum peak current change, obviously,  $[\text{DNA} \cdot \text{DRUG}_m]_{\text{max}} = [\text{DNA}]_0$  holds true. Based on the equations above, the followings can be deduced:

$$\log \frac{\Delta I}{\Delta I_{\text{max}} - \Delta I} = \log K + m \log [\text{DRUG}] \tag{2.8}$$

$$\frac{1}{\Delta I} = \frac{1}{\Delta I_{\text{max}}} + \frac{1}{K \cdot \Delta I_{\text{max}}} \cdot \frac{1}{[\text{DRUG}]^m} \tag{2.9}$$

To Eq. [2.8], we assume  $m=1, 2, 3$ , plot  $\left(\frac{1}{\Delta I}\right) - \left(\frac{1}{[\text{DRUG}]^m}\right)$ , only when  $m=1$ , showed a good linear relationship, and  $\Delta I_{\text{max}}$  calculated is approximate to the experiment data, the assumptive value of  $m$  is reasonable.

Thus, we got Eq. [A.1]

$$\frac{1}{\Delta I_p} = \frac{1}{\Delta I_{p,\text{max}}} + \frac{1}{K \cdot \Delta I_{p,\text{max}}} \cdot \frac{1}{[C]} \tag{A.1}$$

Where  $\Delta I_p$  and  $\Delta I_{p,\text{max}}$  are the difference and the maximum difference of the reduction peak current in the absence and presence of DNA respectively, and  $[C]$  is the concentration of (R)-A or (S)-A added.

**Table 1.** The binding constants ( $K$ ) and the binding free energies ( $E$ ) between (R)-A/(S)-A and DNA

Compounds	$K$ (L·mol <sup>-1</sup> )	$E \times 10^4$ (J·mol <sup>-1</sup> )	
		PBTOT <sup>a</sup>	GBTOT <sup>a</sup>
(R)-A	4255	-2.601	-6.514
(S)-A	623	-1.993	-5.953

<sup>a</sup> The two styles of the binding free energies: PBTOT and GBTOT.[27]

This equation shows that a plot of  $\frac{1}{\Delta I_p}$  versus  $\frac{1}{[C]}$ , if the adsorption process obeys Langmuir adsorption behavior, is a straight line with  $\frac{1}{K \cdot \Delta I_{p, \max}}$  as the slope (Fig. 3 and Fig. 4). The binding constant ( $K$ ) are  $4.255 \times 10^3 \text{ L} \cdot \text{mol}^{-1}$  and  $6.23 \times 10^2 \text{ L} \cdot \text{mol}^{-1}$  for (R)-A/(S)-A, respectively. As listed in Table 1.

The binding constant of (R)-A with CT-DNA is 6.8-fold greater than that of (S)-A, which indicates that the DNA-binding strength of (R)-A is much stronger than that of (S)-A. These results confirm that CT-DNA selectively binds to enantiomer (R)-A. [4] We may speculate that (R)-A could be a more promising drug than (S)-A in cancer treatments.

### 3.2. Molecular docking calculation

It is well known that the interactions of chemical species with the minor groove of DNA differ from those occurring in the major groove, both in terms of electrostatic potential and steric effects, because of the narrow shape of the former. Small molecules interact with the minor groove, while large molecules tend to recognize the major groove binding site. In an effort to interpret the molecular mechanism for interactions of (R)-A/(S)-A with DNA, molecular docking calculation was performed to simulate the modes of interactions between the drugs and DNA. As a result of this interaction, it can be learned from the results of 12 sets that almost all the binding sites of (R)-A/(S)-A were located in the groove of double-helix DNA. Thus, the (R)-A/(S)-A molecule was relatively easy to bind with the minor groove of the duplex DNA with a certain preference of the binding of the cytosine base. [28, 29] Numerous hydrogen bonding and electrostatic interactions occur between a drug and DNA bases and its phosphate backbone. As shown in Fig. 5. Structures of the drug–DNA complexes were predicted on the basis of docking results, where there is a hydrogen bond formed between (R)-A with DNA (Fig. 5A). This is formed between (R)-A and number eight thymine of a chain of DNA, with N atom serving as a hydrogen bond donor (N(10)—H...O(2): 2.66078 Å). As shown in Fig. 5B, similarly, there is a hydrogen bond formed between (S)-A and number six adenine of a chain of DNA, with N atom serving as a hydrogen bond donor (N(11)—H...O(4): 2.85207 Å).

The calculation results indicate that the (R)-A binding with DNA is much more stable than that of (S)-A. It also shows that (R)-A/(S)-A fit snugly into the curved contour of the targeted DNA in the minor groove. Thus, it is a sounding conclusion that the modes of interactions between two prodrugs and DNA helix could be considered as minor groove binding. In order to quantify the binding ability of the (R)-A/(S)-A with DNA, the binding free energy between (R)-A/(S)-A and DNA were calculated. The PBTOT and the GBTOT of the binding free energy between (R)-A and DNA are  $-2.601 \times 10^4 \text{ J} \cdot \text{mol}^{-1}$  and  $-6.514 \times 10^4 \text{ J} \cdot \text{mol}^{-1}$ . As for (S)-A and DNA, the PBTOT and the GBTOT are  $-1.993 \times 10^4 \text{ J} \cdot \text{mol}^{-1}$  and  $-5.953 \times 10^4 \text{ J} \cdot \text{mol}^{-1}$ .

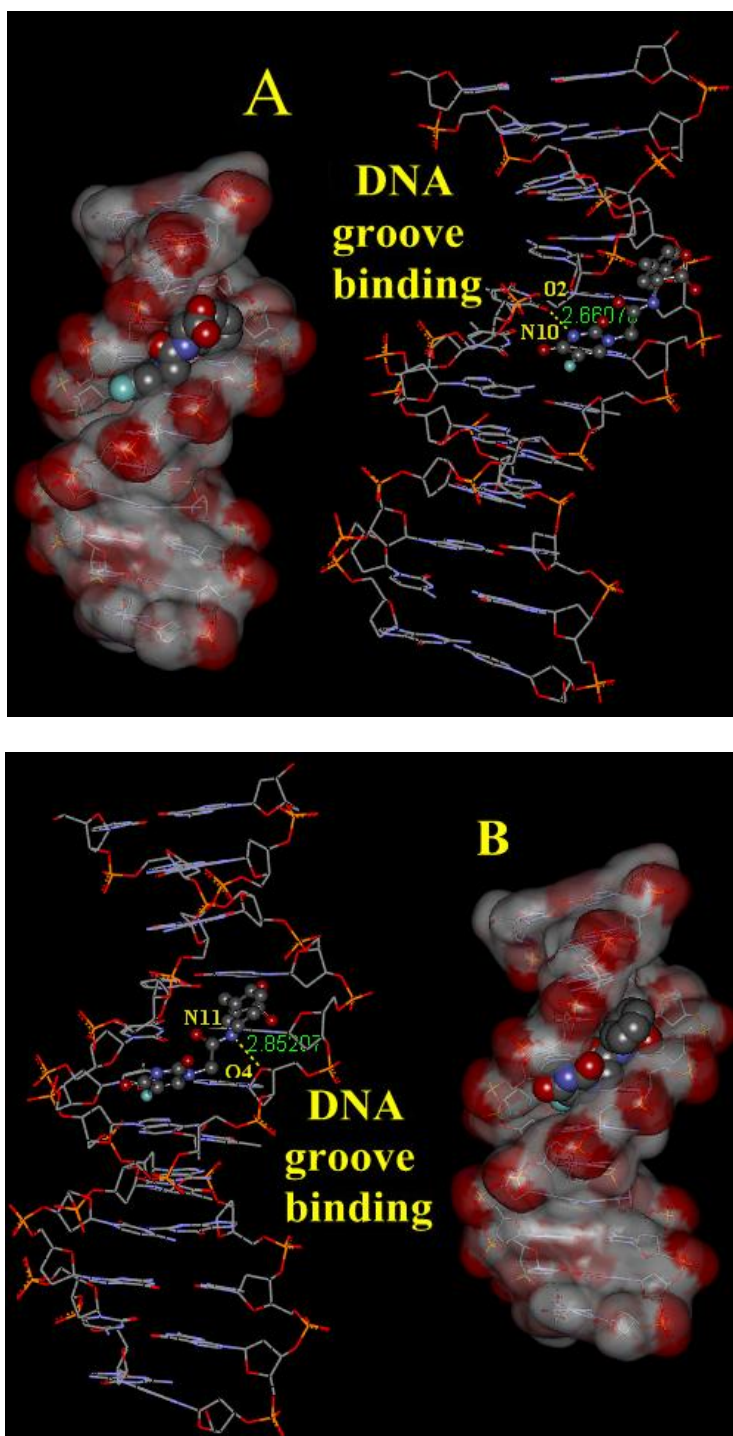


**Figure 5.** A and B illustration of (R)-A/(S)-A binding into DNA, respectively.

As shown in Table 1, the binding free energy of (R)-A is much lower than those of (S)-A. Lower binding free energy indicates a more stable combination with DNA. So, we can conclude that DNA more efficiently binds to (R)-A, and the computational results complement the experimental results. This study serves as a good reference for the process of designing and screening this family of enantiomer prodrugs of 5-fluorouracil.

#### 4. CONCLUSIONS

In this work, the selective interactions of (R)-A/(S)-A with DNA have been investigated using experimental cyclic voltammetry and molecular docking calculation. The results demonstrate that their binding to DNA acts like groove binder which binds to the minor groove of DNA double helix. From the binding constants and the binding free energies, it can be concluded that the binding strength of (R)-A is much stronger than that of (S)-A, the double helical DNA selectively binds to the (R)-A. After all, this study suggests that cyclic voltammetry and molecular docking calculation together are a promising approach for characterizing the mechanism of DNA interaction with targeting compounds, and can serve as a good reference for the rational design and efficient screening enantiomer prodrugs of 5-fluorouracil.

#### ACKNOWLEDGMENTS

This research is supported by the Natural Science Foundation of China (Nos. 21071111 and 21371137) and Commonweal Project of Science and Technology Department of Zhejiang Province (No. 2012C37010).

#### References

1. B. Wang, J. Tan, L. Zhu, *Colloid surface B*. 79 (2010) 1
2. Z. Li, J.H. Tan, J.H. He, Y. Long, T.M. Ou, D. Li, L.Q. Gu, Z.S. Huang, *Eur. J. Med. Chem.* 47 (2012) 299
3. Z.G. Gu, J.J. Na, F.F. Bao, X.X. Xu, W. Zhou, C.Y. Pang, Z. Li, *Polyhedron*. 51 (2013) 186
4. Y. Xu, Y.X. Zhang, H. Sugiyama, T. Umamo, *J. Am. Chem. Soc.* 126 (2004) 6566
5. T. Gu, Y. Hasebe, *Biosens & bioelectron.* 33 (2012) 222
6. A.T. Garcia-Sosa, S. Sild, K. Takkis, U. Maran, *J. Chem. Inf. Model.* 51 (2011) 2595
7. K. Onodera, K. Satou, H. Hirota, *J. Chem. Inf. Model.* 47 (2007) 1609
8. M.L. Verdonk, I. Giangreco, R.J. Hall, O. Korb, P.N. Mortenson, C.W. Murray, *J. Med. Chem.* 54 (2011) 5422
9. Y. Lu, R. Wang, S. Wang, *J. Med. Chem.* 46 (2003) 2287
10. C. Heidelberger, P. Danneberg, D. Mooren, J. Scheiner, *Nature*. 179 (1957) 663
11. D. Garg, S. Henrich, O.M. Salo-Ahen, H. Mylly-kallio, M.P. Costi, R.C. Wade, *J. Med. Chem.* 53 (2010) 6539
12. A. Conejo-Garcia, C.J. Schofield, *Bioorg & Med. Chem. Lett.* 15 (2005) 4004
13. D.B. Longley, D.P. Harkin, P.G. Johnston, D.B. Longley, D.P. Harkin, P.G. Johnston, *Nat. Rev. Cancer*. 5 (2003) 330
14. K.B. Lipkowitz, Y.Y. Fang, E. C. Long, *J. Chem. Theory Comput.* 2 (2006) 1453
15. D.W. Pang, H.D. Abruna, *Anal. Chem.* 70 (1998) 3162
16. M.L. Hu, P. Yin, Z.C. Ma, A. Morsali, *J. Chem Crystallogr.* 38 (2008) 807
17. W.Y. Liu, K.J. Zhang, *Int. J. Electrochem. Sci.* 6 (2011) 1669
18. G.M. Morris, R. Huey, W. Lindstrom, M.F. Sanner, R.K. Belew, D.S. Goodsell, A.J. Olson, *J. Comput. Chem.* 30 (2009) 2785
19. P. Yin, M.L. Hu, X.W. Yan, S. Wang, *Acta Chim. Sinica*. 14 (2008) 1693
20. X.C. Li, K.G. Liu, D. A. Qin, C.C. Cheng, M.L. Hu, *J. Mol. Struct.* 1027 (2012) 104
21. N. Shahabadi, S.M. Fili, F. Kheiridoosh, *J. Photoch. photobio. B.* 128 (2013) 20
22. A. Mehdinia, S. H. Kazemi, S. Z. Bathaie, A. Alizadeh, M. Shamsipur, M.F. Mousavi, *Anal. Biochem.* 375 (2008) 331
23. H.Y. Shen, H.M. Zheng, N. Zhu, Y.Q. Liu, J. Gao, *Int. J. Electrochem. Sci.* 5 (2010) 1587

24. H.X. Ju, Y.K. Ye, Y.L. Zhu, *Electrochim. Acta.* 50 (2005) 1361
25. M.H. Banitaba, S.S.H. Davarani, A. Mehdinia, *Anal. Biochem.* 411 (2011) 218
26. F. Qu, N.Q. Li, Y.Y. Jiang, *Talanta.* 45 (1998) 787
27. A.T. Baviskar, C. Madaan, R. Preet, P. Mohapatra, V. Jain, A. Agarwal, S.K. Guchhait, C.N. Kundu, U.C. Banerjee, P.V. Bharatam, *J. Med. Chem.* 54 (2011) 5013
28. R. Gaur, R.A. Khan, S. Tabassum, P. Shah, M.I. Siddiqi, L. Mishra, *J. Photoch. photobio.A.* 220 (2011) 145
29. M.M. Islam, M. Chakraborty, P. Pandya, A.A. Masum, N. Gupta, S. Mukhopadhyay, *Dyes. Pigments.* 99 (2013) 412